Kinetic delay in cooperative supramolecular polymerization by redefining the trade-off relationship between H-bonds and Van der Waals / π- π stacking interactions.

William T. Gallonde, Corentin Poidevin, Felix Houard, Elsa Caytan, Vincent Dorcet, Arnaud Fihey, Kevin Bernot, Stéphane Rigaut, Olivier Galangau

Kinetic delay in cooperative supramolecular polymerization by redefining the trade-off relationship between H-bonds and Van der Waals / π- π stacking interactions.

William T. Gallonde,[a] Corentin Poidevin,[a] Felix Houard,[b] Elsa Caytan,[a] Vincent Dorcet,[a] Arnaud Fihey,*[a] Kevin Bernot,[b] Stéphane Rigaut*[a] and Olivier Galangau*[a]

[a] W. T. Gallonde, C. Poidevin, Dr. E. Caytan, Dr. V. Dorcet, Dr. A. Fihey, Prof. S. Rigaut, Dr. O. Galangau
Univ. Rennes, CNRS, ISCR (Institut des Sciences Chimiques de Rennes) – UMR 6226
35000 Rennes, France
E-mail: arnaud.fihey@univ-rennes.fr, stephane.rigaut@univ-rennes.fr, olivier.galangau@univ-rennes.fr

[b] Dr. F. Houard, Prof. K. Bernot
Univ. Rennes, INSA Rennes, CNRS, ISCR (Institut des Sciences Chimiques de Rennes) – UMR 6226
35000 Rennes, France

Abstract: We here present how rebalancing the interplay between H-bonds and dispersive forces (Van der Waals / π- π stacking) may induce or not the generation of kinetic metastable states. In particular, we show that extending the aromatic content and favouring the interchain VdW interactions causes a delay into the cooperative supramolecular polymerization of a new family of toluene bis-amide derivatives by trapping the metastable inactive state.

Introduction

One dimensional (1D) self-assembly of small molecules *via* supramolecular polymerization provides an appealing route toward (multi)functional (bio)materials, conducting fibers or photo-active nano-assemblies.[1] In those 1D materials, the small molecule monomers are tightly bound together by reversible and highly directional non-covalent interactions, such as dipole-dipole interactions, hydrogen bonds, halogen bonds, π- π stacking or interchain interactions to name a few. [2] Their inherent high dynamicity ensures that the polymeric growth typically occurs under thermodynamic control. Those supramolecular polymers were distinguished into two main categories depending on their self-assembly mechanism. In a step-growth, isodesmic mechanism, monomer aggregation is driven by a single equilibrium constant for each monomer addition, regardless of the aggregate size. Conversely, the ubiquitous cooperative mechanism (nucleation-elongation) features a two-step process, implying first the thermodynamically unfavorable formation of nuclei followed by the much more favorable elongation of the stacks from the nuclei associations. [3] The last decade has revolutionized our understanding of supramolecular polymerizations by introducing kinetic control of their chain growth in very specific cases, the so-called pathway complexity.[4] Kinetic effects do emerge in supramolecular polymerization when monomers are strongly interacting with each other in aggregates, which structure differs from the thermodynamic one, or in an intramolecular way, [5] therefore presenting a rather low dynamicity and affinity for further aggregation. This allows the monomers to be confined into energy traps as dormant states, lying at higher energy than the global thermodynamic minimum state. Whether the dormant state would relax toward an activated state, then to the thermodynamic minimum, will depend on the kinetic barrier that the monomer has to overcome. If this kinetic barrier is small, the dormant state is termed kinetically metastable state.

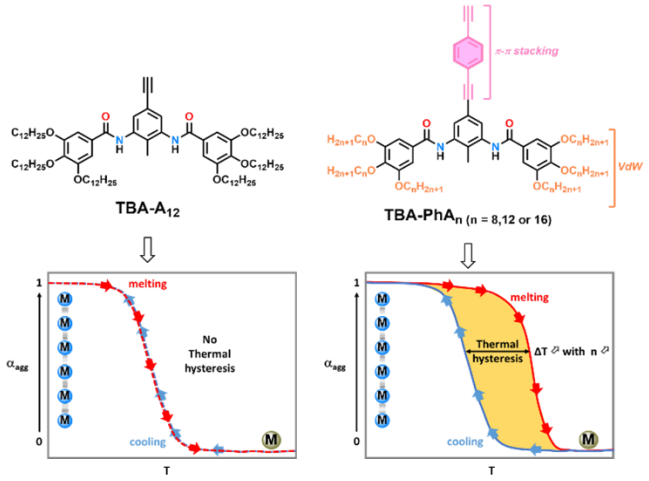

Scheme 1. Molecular structures of compound **TBA-A$_{12}$**, **TBA-PhA$_8$**, **TBA-PhA$_{12}$** and **TBA-PhA$_{16}$**.

To do so, judiciously designed monomers equipped with H-bonding groups that can be engaged into *intramolecular* hydrogen bonding interactions were prepared. [5b] In that case, since the H-bond functional moieties are no longer available, the spontaneous nucleation is delayed, thereby leading to the opening of a thermal hysteresis in the plot of the aggregation parameter α_{agg} *vs* T. In line with this H-bonding strategy, the group of Würthner has recently taken advantage of *intermolecular* H-bonding interactions with a dedicated molecular chaperone to produce kinetically dormant state. [6a] Very recently, Wang et al. [6b] reported the ability of π- π stacking interactions to also promote a kinetically metastable driving the supramolecular assembly of donor-acceptor aromatic molecules. Therefore, it appears that not only H-bonds but dispersion forces play a key role and strategies where such forces with Van der Waals interactions in addition to π-π stacking may prevail over H-bonds. It may also allow the generation of kinetic metastable states. Eventually, the dormant

state would rearrange into a more favorable way, a so-called active state where the H-bonds would take over the dispersive interactions and from which the growth would initiate. Such transit from dormant to active state would very likely delay the polymerization. However, a strategy enabling fine tuning of the thermal hysteresis by dispersive forces interplay is yet to be achieved.

In this work, we specifically demonstrate that precise chemical engineering of dispersive forces balancing hydrogen bonding allows the control of the existence and the characteristics of a dormant state, and *in fine* of the supramolecular polymerization. To reach this goal, we selected toluene bis-amide (TBA) compounds featuring two amide groups *ortho*-positionned with respect to the methyl and are known for decades to efficiently gel organic solvents.[7] Indeed, the amide groups form hydrogen bonding interactions in opposite directions to lead to a molecular packing in a head-to-tail fashion with plane-to-plane distances of approx. 4.2 Å, leading to the formation of 1D fibers. As these compounds can be easily functionalized, with acetylenic or with extended aromatic moieties (Scheme 1), some of us recently used such ligands to self-assemble bulky Ru^{II} bis-acetylide complexes.[8] Herein, we further demonstrate for the first time that (i) the increase of π-π stacking interactions in **TBA-PhA$_{12}$** compared to **TBA-A$_{12}$** and (ii) the regulation of interchain VdW interactions in TBA derivatives functionalized with alkyl side chains of various length from new **TBA-PhA$_{12}$** to new **TBA-PhA$_{16}$** enables not only the control of the kinetic metastable states existence but also operates on the polymerization kinetic barrier to form 1D fibers. The characteristics of this state and of the polymerization process were determined experimentally, in particular with the observations of hysteresis loops, and modeled with the help of theoretical calculations.

Results and Discussion

Synthetic routes to obtain derivatives **TBA-A$_{12}$**, **TBA-PhA$_{12}$** were previously reported,[8,9] and **TBA-PhA$_8$** and **TBA-PhA$_{16}$** encompassing C_8 and C_{16} alkyl chain lengths, respectively, (Scheme 1) were synthetized accordingly (SI).

Investigations of the supramolecular polymerizations of the C$_{12}$ derivatives

In dichloromethane (DCM) the **TBA-A$_{12}$** molecule resides in its monomeric state as proved by FTIR measurements of a 10 mM solution (Figure S38-S39) which indicate a stretching vibration of the N-H group at 3428 cm^{-1} and a stretching vibration of the C=O group at 1679 cm^{-1} that are characteristic of amido groups free from hydrogen bonding interactions. In contrast, measurements of a 10 mM preparation of the same **TBA-A$_{12}$** in MCH affords clear evidences of red shifting of the N-H and C=O stretching vibrations caused by strong intermolecular hydrogen bonding. Further proof of **TBA-A$_{12}$** self-assembly can be obtained from TEM images of drop casted aliquots of a 400 µM preparation in MCH (Figure S44). Micrometer long ribbons characterized by a width ranging from 60 nm to 300 nm and a thickness of around 60 nm resulted from the columnar organization of this molecule. [7a]

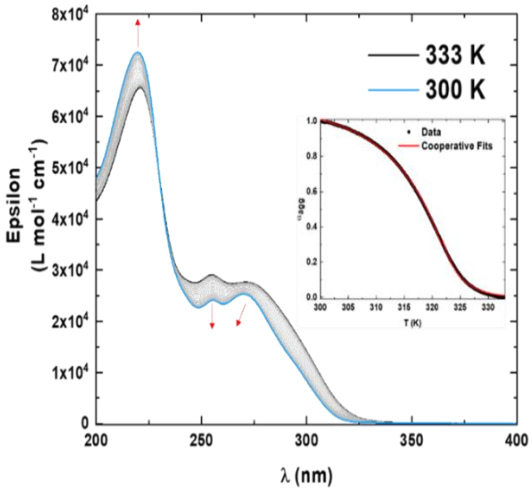

Figure 1. Variable temperature UV/Vis measurement of **TBA-A$_{12}$** in MCH (C_T = 400 µM) between 333 K and 300 K. The inset shows the plotting of the aggregation parameter at 315 nm.

We further investigated **TBA-A$_{12}$** self-assembly properties by means of Temperature-controlled spectrophotometric measurements (Figure 1). At 333 K, the absorption spectrum superimposes well with that of the molecule dissolved in DCM (Figure S25) confirming that the molecule lies in its free monomeric state. Upon cooling the same solution at a rate of 1 K/min, the bands located at approx. 250 nm and 300 nm experience a blue shift concomitantly with a decrease in optical density in line with the formation of out of plane H-bonds leading to a decrease of conjugation between the toluene fragment and the amide one. Meanwhile, the band peaking at 225 nm increases, yielding a pseudo-isobestic point located at approximatively 230 nm. Upon warming up the sample, the observed absorption changes are fully reversible. Plotting the aggregation parameter at 315 nm *versus* T affords a clear non-sigmoïdal curve symptomatic of cooperative supramolecular polymerizations. The cooperativity of this process clearly relates to strong directional hydrogen bonds running in opposite direction, as suggested by Ghadiri and coworkers[10] for cyclic peptides and to some extent to π-π stacking interactions in the present case. Of great interest is the fact that both cooling and melting processes afford superimposable (Figure S27) curves suggesting that in those experimental conditions **TBA-A$_{12}$** is under full thermodynamic control. Using the fitting functions reported by Meijer and co-workers[11] for cooperative growth affords a significant elongation enthalpy (ΔH_e) of - 138 kJ mol^{-1} and an elongation entropy (ΔS_e) of -360 J K^{-1} mol^{-1}, confirming that the supramolecular polymerization is enthalpically driven. The model also yields activation constant (K_a) values at the elongation temperature (Figure S26 and Table S1) close to 8×10^{-3}, supporting the observed cooperativity of the system. Interestingly, these values are close to the ones found by Meijer et al.[11] for *C_3*–symmetric OPE scaffolds.

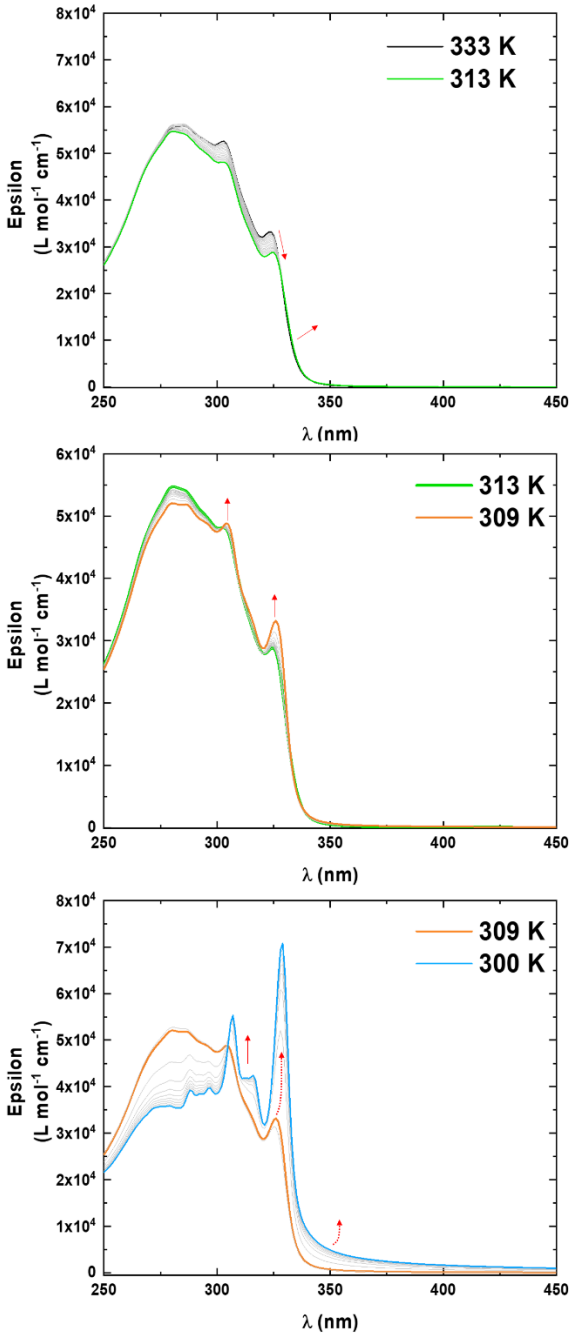

Figure 2. Variable temperature spectrophotometric measurement upon cooling of **TBA-PhA$_{12}$** in MCH (C_T = 370 µM) between 333 K and 313 K (top), 313 K and 309 K (middle) and 309 K and 300 K (bottom). The red arrows indicate the variation of the absorption spectra.

Now turning to derivative **TBA-PhA$_{12}$**, which entails an elongated aromatic platform compared to the previous molecule, we could observed, in DCM (C_T = 10 mM) at room temperature, a FTIR spectrum featuring characteristic stretching vibration bands of free N-H and C=O bonds at 3424 cm^{-1} and 1676 cm^{-1}, respectively (Figure S40). These values strongly suggest that in DCM the molecule remains in its monomeric state. In contrast, **TBA-PhA$_{12}$** is known to form organogels in MCH, thanks to strong hydrogen bonding interactions.[8] This is undoubtedly confirmed by the FTIR spectrum at room temperature (C_T = 10 mM) where the stretching vibration bands of N-H and C=O experience a dramatic red shift down to 3155 cm^{-1} and 1636 cm^{-1}, respectively (Figure S41).

The nature of the as-formed aggregates was confirmed by TEM and AFM measurements (Figure S45). **TBA-PhA$_{12}$** forms 1D micrometer long supramolecular ribbons, smaller than that of **TBA-A$_{12}$**, with characteristic width of 10 nm to 80 nm and thickness of 20 nm that are responsible for the gelation of MCH at concentration higher than the critical gel concentration. We have further conducted variable temperature spectrophotometric measurements in MCH from 333K to 300 K. In stark contrast to **TBA-A$_{12}$**, **TBA-PhA$_{12}$** displays a rather complex behavior, which can be decomposed into several steps (Figure 2). At temperatures above 323 K, the absorption spectrum overlaps well with the spectrum of the molecule dissolved in DCM at room temperature (Figure S29), meaning that at 333 K, the molecule lies in its free monomeric state. This is also supported by the 2D NOESY experiments at the same temperature, which do not detect any intermolecular interactions.

At this highest temperature and for a total concentration of 370 µM, the absorption spectrum of monomeric **TBA-PhA$_{12}$** (black line) features a first band located at 325 nm and a second peaking at 303 nm. Upon cooling at a rate of 1 K/min and down to 313 K, the band at 325 nm undergoes a decrease in intensity accompanied by a slight red shift to 328 nm. This suggests that the monomers undergo a first supramolecular process leading to a new intermediate aggregate. From 313 K to 309 K, a new absorption pattern appears with the growing at 326 nm of a novel and narrower band suggesting the emergence of a second intermediate specie. The appearance of a pseudo-isobestic point located at 302 nm plainly suggests a clean transition from one molecular arrangement to another one. Eventually, upon further cooling, starts the growth of a well-structured absorption fingerprint featuring maxima at 329 nm, 316 nm and 307 nm assigned to the formation of the 1D supramolecular polymers. Interestingly, this growth is also accompanied by the formation of a pseudo-isobestic point located at 305 nm. Upon warming the solution, these spectral changes are reversible yet with a sizeable thermal shift of approx. 8 K. This is readily quantified by plotting the aggregation parameter at 350 nm *vs* temperature for several concentrations (Figure 3). In addition, lowering the temperature rate (0.1 K/min instead of 1 K/min) does not have any effect either (Figure S32).

This thermal hysteresis, strongly suggest that **TBA-PhA$_{12}$** undergoes a kinetically controlled cooling process, while its melting is under thermodynamic control.[13] Accordingly, we surmise that upon cooling, **TBA-PhA$_{12}$** monomers undergo a first process leading to the formation of a kinetic metastable state (green absorption spectrum). This metastable state then evolves toward an active state (orange spectrum) from which the polymerization can start. Since the thermal hysteresis width directly relates to the energy barrier that traps the metastable state,[13g] we imagine this kinetic barrier should be very small.

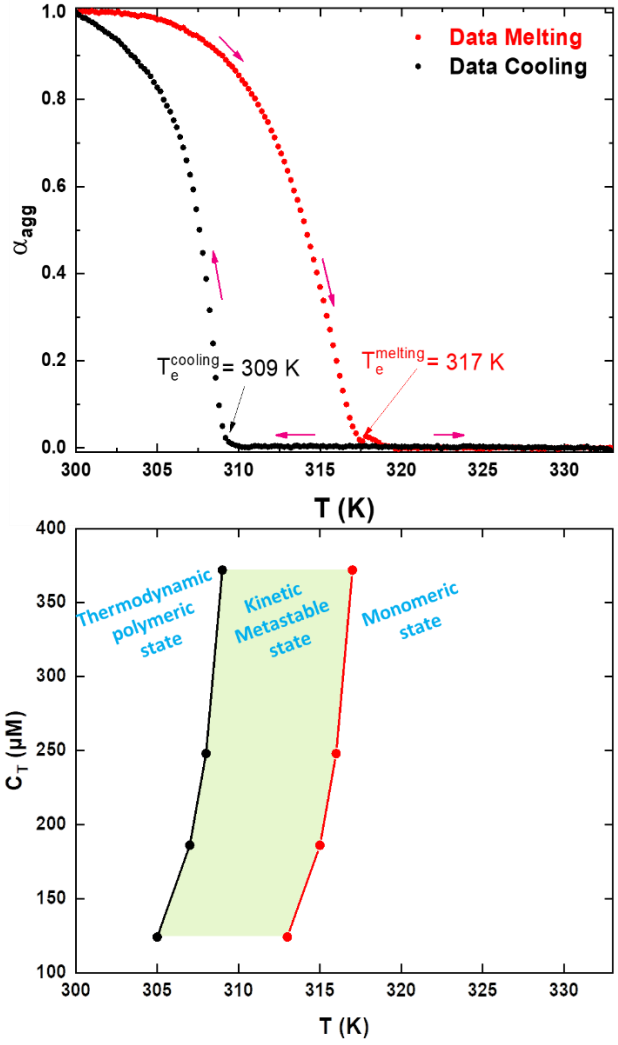

Figure 3. (Top) Example of thermal hysteresis observed for **TBA-PhA$_{12}$** (C_T = 370 µM). (Bottom) thermal hystereses for different concentrations.

Investigations of the thermodynamic aggregate of TBA-PhA$_{12}$. The non-sigmoidal profile of the aggregation parameter *vs* temperature plot as well as the excellent agreement of the cooperative model clearly indicate that **TBA-PhA$_{12}$** forms 1D aggregate thanks to a cooperative nucleation / elongation mechanism (Figure S30 and Table S2). The pseudo Van't Hoff plot yields ΔH_e of - 216 kJ mol^{-1} and ΔS_e of -632 J K^{-1} mol^{-1} in perfect agreement with an enthalpically driven aggregation process. To the best of our knowledge, such an enthalpy release is among the highest so far reported, and recalls the slightly less negative enthalpy release values measured with oligo(phenylene-ethylene)s by Meijer et al. [12] The K_a value was determined to be 2×10^{-3}, indicating a slight improvement of the cooperativity when elongating the molecular scaffold compared to **TBA-A$_{12}$**.

We further investigated the thermodynamic packing by monitoring the melting (1 K/min) of **TBA-PhA$_{12}$** 1D aggregates ($MCHd_{14}$, C_T = 10 mM) by means of variable temperature ^{1}H NMR (Figure 4). At such concentration, the solution turned out to be a translucent gel from 298 K to 322 K, hence leading to poorly resolved spectra, symptomatic of strong aggregation. Further warming allows one to recover the characteristic molecular signals. In particular, the broad signal located at 8.4 ppm, assigned to the amido protons, experienced an upfield shift upon warming, confirming that hydrogen bonds are partly responsible for the self-assembly of **TBA-PhA$_{12}$**. Upon increasing the temperature, the downfield variations of the Me signal (H_{Me}) of the toluyl fragment aromatic proton (H_{Tol}) and of the protons located on the phenyl acetylene (H_a, H_b) moiety conclusively suggest **TBA-PhA$_{12}$** molecules most likely pack via π-π stacking. To complete our view, we have performed 2D NOESY experiments at 333 K (monomeric state) and 328 K (aggregate state). The 2D NOESY spectrum at the highest temperature displayed cross-correlations that are of intramolecular nature. At 328 K, new correlation spots appeared. A first one indicates that the alkyl chains lie close to the alkynyl proton (Figure S23). Besides, a weak correlation was found between H_b and H_{Me} strongly suggesting that **TBA-PhA$_{12}$** packs in a *head-to-tail* fashion (Figure 4a). Correlations between the H_a and H_b signals and the methylenic protons OCH_2 (Figure 4b) were also observed stressing the fact the phenyl-acetylene moiety clearly interacts with the gallic parts of a neighboring molecule, stabilizing the *head-to-tail* supramolecular architectures in line with the increase of enthalpy release of elongation when going from **TBA-A$_{12}$** to **TBA-PhA$_{12}$**. This clearly underlines the strong contribution of π- π stacking interactions into the thermodynamic supramolecular packing, more likely to a *twisted head-to-tail* arrangement (*vide infra*).

Investigations of the kinetic metastable state of TBA-PhA$_{12}$. Following the work of Würthner *et al.*,[13b] we aimed at monitoring the aggregate growth at 328 nm, as a function of time, after a fast cooling step (20 K/min) from 333 K to a chosen final temperature to trap the kinetic state. When the final temperature was below the hysteresis limit (305 K), the aggregation was extremely fast and ended in few hundreds of seconds (Figure S36), as one could expect. We selected 310 K (C_T = 370 µM), since the aggregation is much slower by taking a bit more than 2 hours to reach completion, and then recorded the kinetic profiles for various concentrations (Figure 5). Note that this non-sigmoidal profile of the curves ($\Delta\varepsilon$ vs. t) is characteristic of a slow continuous nucleation followed by autocatalytic (burst) growth.[14] In addition, decreasing the concentration results in increasing the aggregation lag time. This is in line with an ON-pathway mechanism[13b] involving that the metastable state consecutively leads to the formation of an active state which structure authorizes the nucleation to occur. However, we failed to isolate or observe the kinetically metastable state by TEM or AFM. Therefore, we performed variable temperature dynamic light scattering experiments, hoping to detect the formation of such metastable aggregate state (Figure S50). At 333 K, a scattering intensity close to 0 was obtained in line with the fact that the molecule resides in its free monomeric state. Cooling the sample at 20 K/min to 300 K (below the thermal hysteresis boundary) induces a marked increase of the scattering intensity because of the growth of the 1D supramolecular polymers. We repeated the same experiment stopping at 310 K with C_T =190 µM trapping the kinetically metastable state for at least 5 hours. No significant

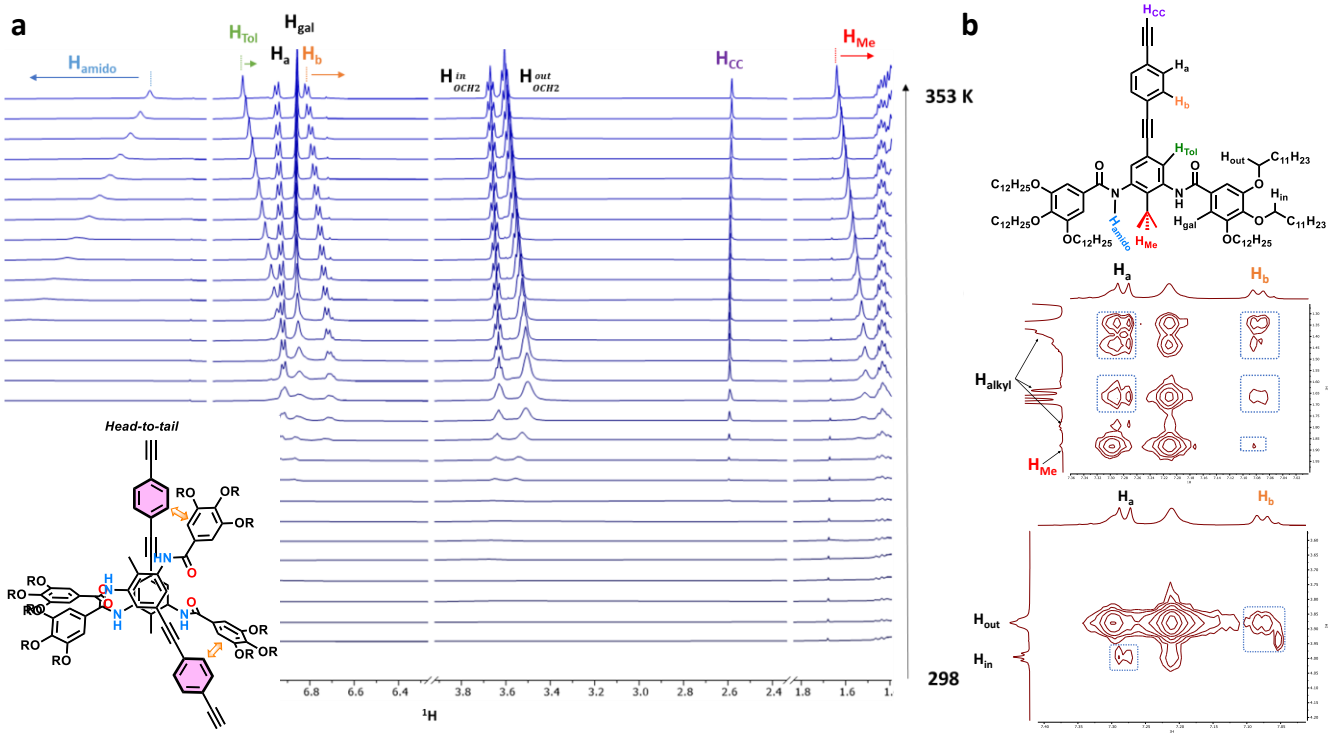

Figure 4. a) Partial ^{1}H VT-NMR spectra of **TBA-PhA$_{12}$**. b) Molecular structure of **TBA-PhA$_{12}$** indicating the different protons and c) partial 2D NOESY correlations found at 328 K (aggregate state) indicating the interactions between the phenyl-acetylene moiety in **TBA-PhA$_{12}$** and the gallic parts of a neighboring molecule.

increase of scattering intensity was observed, and this suggest that the kinetically formed aggregate is too small to be observed. The resolution of our VT-DLS setup is 0.5 nm meaning that the kinetically metastable state should involve an aggregate with a characteristic size inferior or equal to 5 Å. Such dimensions impose us to consider dimeric structures of **TBA-PhA$_{12}$** (*vide infra*). This is further supported by the fitting of the kinetic profiles at C_T = 370 µM and C_T = 340 µM using Amylofit[15] which agrees well with an unseeded nucleation – elongation growth characterized by a nucleus size of 2 (see SI & Figure S57).

Investigations of the supramolecular polymerization of the C$_8$ and C$_{16}$ derivative

Whereas NMR and IR spectroscopy allows to get relevant informations on hydrogen bonding and π-π stacking interactions, the role of aliphanic chains remains unclear in this process. In order to better delineate the role of the aliphatic side chains and the importance of VdW interactions, in particular in the formation of the kinetic metastable state, we investigated the supramolecular polymerizations in MCH of the two analogousderivatives **TBA-PhA$_8$** and **TBA-PhA$_{16}$**, featuring either C_8 or C_{16} alkyl chains, respectively. It appears that both derivatives also form 1D supramolecular aggregates in MCH at room temperature as seen by TEM (Figures S46-S47). While **TBA-PhA$_8$** formed stiff ribbons, **TBA-PhA$_{16}$** aggregated in long and flexible ribbons like **TBA-PhA$_{12}$**. We further performed VT UV/vis experiments on both compounds. Unfortunately, cooling a MCH solution of **TBA-PhA$_8$** led to the formation of a precipitate and the characteristic band assigned to the 1D thermodynamic aggregate was not observed. We assigned this to the lack of solubility of **TBA-PhA$_8$** supramolecular aggregates because of the shortening of the alkyl chains. In contrast, **TBA-PhA$_{16}$** yielded results that were similar to those found for **TBA-PhA$_{12}$**. Indeed, the spectral signature of the thermodynamic aggregates of **TBA-PhA$_{16}$** matches the one of **TBA-PhA$_{12}$**, indicating (i) the presence of a kinetically metastable state with the appearance of a marked thermal hysteresis of 16 K, twice the one of **TBA-PhA$_{12}$,** and (ii) that thermodynamic packing is probably also of *twisted head-to-tail* nature. More importantly, these results highlight that redefining the trade-off relationship between π-π stacking, H-bonding and VdW interactions may significantly influence the presence and the nature of a kinetically dormant state.

Computational investigations of the steps of TBA-PhA$_{12}$ supramolecular polymerizations

To investigate the geometric nature of the kinetic metastable state, we have performed a conformational theoretical study on a simplified monomer where the C_{12} chains were replaced by CH_3 groups (see supporting information for more details and a full methodology). As suggested by DLS experiments, we first computed several possible conformations for *dimeric* structures of **TBA-PhA$_{12}$**.

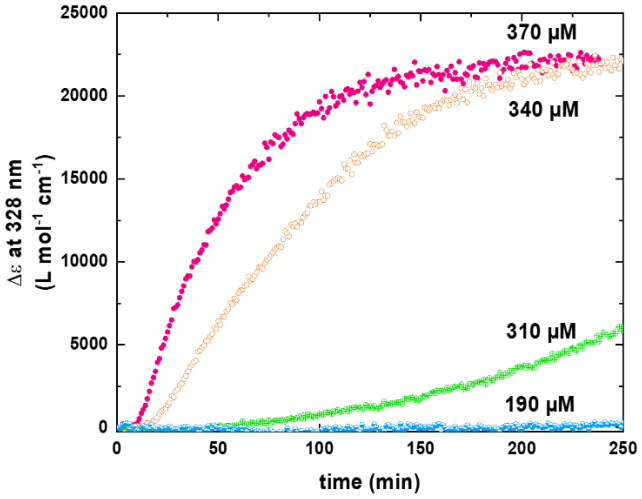

Figure 5. Kinetic profiles of the aggregation growth with **TBA-PhA$_{12}$** monitored at 310 K, after fast cooling (20 K/min) from 333 K.

Molecular Dynamic (MD) followed by geometry optimizations have yielded two most stable dimers, namely D1 and D2 (Figure 6). D1 features a *twisted head-to-tail* packing while D2 displays a *face-to-face* arrangement. Although D1 shows stronger H-bonds with a mean distance of 2.04 Å (Table 1) than D2 (2.28 Å), the latter is predicted to be more stable than D1 by 5 kJ mol^{-1}. Such an increase in stability is likely related to the π-π stacking interactions between the two phenyl-ethynyl fragments in D2 that are prevailing over H-bonding interactions. However, the *twisted head-to-tail* packing becomes more favorable when further moving to a trimer (Figure S27 & Table 1), where T1 featuring a *twisted head-to-tail* packing is much more stable than T2,which relies on a *face-to-face* arrangement, by 41 kJ mol^{-1}.

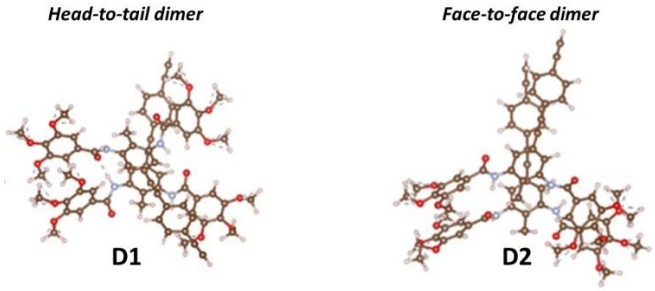

Figure 6. Optimized geometries of the most stable dimeric structures D1 and D2.

Consequently, we propose that **TBA-PhA$_{12}$** undergoes a first *face-to-face* dimerization, inhibiting the formation of the favorable *head-to-tail* nuclei. Indeed, the dimer conformation has to transit from *face-to-face* dormant state to *twisted head-to-tail* active state so the cooperative supramolecular polymerization could start, which is likely causing the observed experimental delay.

	DLPNO-CCSD(T)	Mean H-bond (Å)
D2	**-45.0**	**2.28**
D1	**-40.0**	**2.04**
T2	**-53.8**	2.26/2.75
T1	**-95.3**	2.25/3.75

Table 1. Relative energies in kJ/mol of the calculated structures optimized at the r2SCAN-3c level and with single point calculations at the DLPNO-CCSD(T)/cc-pVTZ level. Mean H-bond distances in Å between two monomers.

Further theoretical evidences can help deciphering the behavior of **TBA-PhA$_{12}$**. We computed UV-visible spectra of the monomer and the dimers D1 and D2. We have plotted (Figure 7) the sum of the UV-visible spectra of the monomer and of one of the conformations (D1 or D2) of the dimer with increasing weight of the dimers (from 100 percent monomer to 60 percent). This study thus reveals that an increase of the *head-to-tail* dimer population D1 within the solution should lead to the emergence of a growing band located in the blue part of the absorption spectrum (~245 nm), while a decrease of the absorption in the red part of the spectrum (~270 nm) should be observed for an increase of the *face-to-face* D2 population. Despite the fact that the calculated spectrum of the monomer is slightly blue shifted compared to experiment probably owing to the computational method with and the absence of solvent effects.[16] only the latter situation corresponds to the experimental observations (Figure 2 top), thereby further supporting the fact that the *face-to-face* D2 packing is accessed prior to the *head-to-tail* D1.

To sum up, all these results suggest the energetic profile described in Scheme 2 for the supramolecular polymerization of **TBA-PhA$_n$**. Upon cooling, the monomer undergoes a dimerization process leading first to a *face-to-face* packing, driven mainly by dispersive interactions, which inhibits the cooperative growth. Conformational change from *face-to-face* to *twisted head-to-tail* requires disrupting the π–π stacking and the VdW interactions resulting in an energetic barrier able to trap this state. Increasing the VdW contributions by extending the side-chains from C_{12} to C_{16} causes the barrier increase with a widening of the thermal hysteresis, therefore allowing a fine control of the polymerization dynamic. After conformational change, the *head-to-tail* dimer initiates the nucleation / elongation growth leading to the formation of the supramolecular fibers.

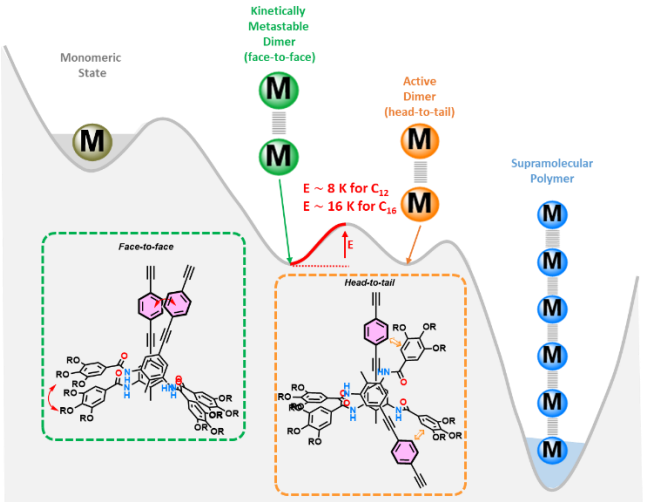

Scheme 2. Proposed mechanism of self-assembly for **TBA-PhA$_{12/16}$. R = $C_{12}H_{25}$ or $C_{16}H_{33}$.**

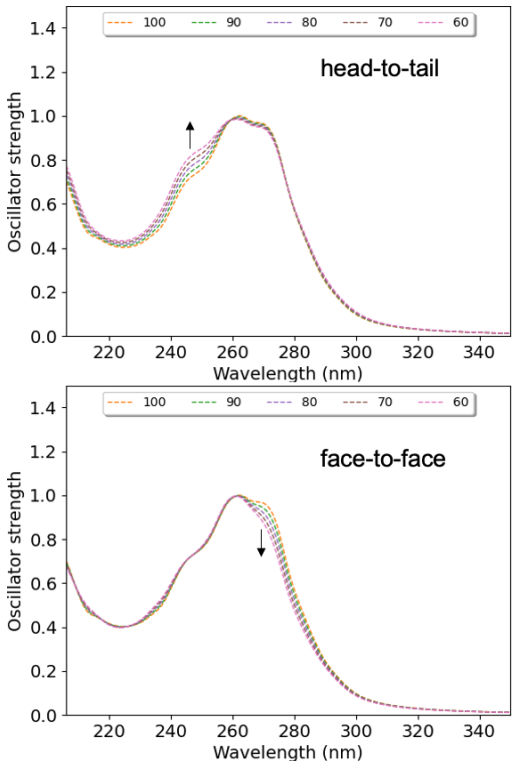

Figure 7. Normalized UV-Visible spectra computed at the LC-DFTB2 level from 100 MD snapshots of the a 100, 90, 80, 70 and 60 percent of monomer and 0, 10, 20, 30 and 40 percent of the dimer in *head-to-tail* (top) and *face-to-face* (bottom) configuration, respectively. See SI for computational details. The arrow indicates the absorption change as the dimer population increases.

Conclusion

In this work, we have investigated the 1D self-assembly of a series of representative molecules from the Toluene Bis-Amide family. We proved experimentally and with theoretical support that rebalancing the cooperation between π–π stacking, interchain VdW interactions and H-bonds by increasing the relative strength of the dispersive forces may trigger the existence of a kinetically metastable state, allowing minute tailoring of the corresponding dormant state and the control of the cooperative supramolecular polymerization kinetic. This work also highlights that careful design of aromatic systems can also be a tool for kinetically control cooperative polymerizations. We are currently investigating seed-assisted polymeric growth to gain further pathway control. We believe that such work is of interest for the community and could be generalized to other appropriate molecular scaffold.

Acknowledgements

Part of this work has been performed using NMR spectrometer(s) belonging to the PRISM Multimodal Imaging and Spectroscopy Research Platform (Biogenouest©, UMS Biosit, Université de Rennes). The authors thank J-F. Bergamini for his help in recording AFM data. The authors thank the THEMIS Platform (ScanMAT - UAR2025) for TEM facilities access. The authors thanks the Université de Rennes, Rennes Métropôle, the CNRS and the ANR (SAMAT, ANR-21-CE06-0012-01). A. Fihey and C. Poidevin are grateful for the support of the ANR through the FALCON project (grant ANR-20-CE09-0002-01).

Keywords: Self-assembly • Supramolecular polymer • hydrogen bonding • cooperativity • pathway complexity

[1] a) F. Xu, Ben L. Feringa, *Adv.Mater.* **2023**, 2204413 and references therein; b) T. Fukushima, K. Tamaki, A. Isobe, T. Hirose, N. Shimizu, H. Takagi, R. Haruki, S. Adachi, M. J. Hollamby, S. Yagai, *J. Am. Chem. Soc.* **2021**, *143*, 5845-5854; c) Z. Gao, Y. Han, F. Wang, *Nat. Commun.* ***2018***, *9*, 3977; d) V. Faramarzi, F. Niess, E. Moulin, M. Maaloum, J-F. Dayen, J-B. Beaufrand, S. Zanettini, B. Doudin, N. Giuseppone *Nat. Chem.* ***2012***, *4*, 485-490. e) O. J. G. Goor, S. I. S. Hendrikse, P. Y. W. Dankers, E. W. Meijer *Chem. Soc. Rev.* **2017**, *46*, 6621-6637. f) M. Hasegawa, M. Iyoda *Chem. Soc. Rev.* **2010**, *39*, 2420-2427.

[2] a) T. F. A. De Greef, M. M. J. Smulders, M. Wolffs, A. P. H. J. Schenning, R. P. Sijbesma, E. W. Meijer, *Chem. Rev.* **2009**, *109*, 5687-5754 and references therein; b) T. Aida, E. W. Meijer, *Isr. J. Chem.* **2020**, *60*, 33-47; c) P. K. Hashim, J. Bergueiro, E. W. Meijer, T. Aida, *Prog. Polym. Sci.* ***2020***, *105*, 101250 and references therein.

[3] a) C. Rest, R. Kandanelli, G. Fernandez, *Chem. Soc. Rev.* **2015**, *44*, 2543-2572 and references therein; b) C. Kulkarni, E. W. Meijer, A. R. A. Palmans, *Acc. Chem. Res.* **2017**, *50*, 1928-1936; c) M. Hartlieb, E. D. H. Mansfield, S. Perrier, *Polym. Chem.* ***2020***, *11*, 1083-1110 and references therein; d) M. Wehner, F. Würthner, *Nat. Rev. Chem.* ***2020***, *4*, 38-53 and references therein.

[4] a) P. A. Korevaar, S. J. George, A. J. Markvoort, M. M. J. Smulders, P. A. J. Hilbers, A. P. H. Schenning, T. F. A. De Greef, E. W. Meijer, *Nature* **2012**, *481*, 492-497; b) P. A. Korevaar, T. F. A. De Greef, E. W. Meijer, *Chem. Mater.* **2014**, *26*, 576-586.

[5] a) G. Ghosh, P. Dey, S. Ghosh, *Chem. Commun.* **2020**, *56*, 6757-6769 and references therein; b) S. Dhiman, S. J. George, *Bull. Chem. Soc. Jpn.* ***2018***, *91*, 687-699. c) M. Endo, T. Fukui, S. H. Jung, S. Yagai, M. Takeuchi, K. Sugiyasu, *J. Am. Chem. Soc.* **2016**, 138, 14347-14353

[6] a) L. Kleine-Kleffmann, V. Stepanenko, K. Shoyama, M. Wehner, F. Würthner, *J. Am. Chem. Soc.* **2023**, 145, 9144-9151; b) F. Wang, R. Liao, F. Wang, *Angew. Chem. Int. Ed.* **2023**, e202305827.

[7] F. Camerel, L. Bonardi, G. Ulrich, L. Charbonnière, B. Donnio, C. Bourgogne, D. Guillon, P. Retailleau, R. Ziessel, *Chem. Mater.* **2006**, *18*, 5009-5021.

[8] a) O. Galangau, E. Caytan, William T Gallonde, I. de Waele, F. Camerel, S. Rigaut, *Eur. J. Inorg. Chem.* **2022**, e202200579; b) O. Galangau, D. Daou, N. El Beyrouti, E. Caytan, C. Mériadec, F. Artzner, S. Rigaut, *Inorg. Chem.* **2021**, *60*, 11474-11484.

[9] F. Camerel, G. Ulrich, R. Ziessel, *Org. Lett.* **2004**, 6, 4171-4174.

[10] M. R. Ghadiri, J. R. Granja, R. A. Milligan, D. E. McRee, N. Khazanovich, *Nature* **1993**, 366, 324-327.

[11] P. Jonkheijm, P. Van der Schoot, A. P. H. J. Schenning, E. W. Meijer, *Science* **2006**, 7, 5783.

[12] F. Wang, M. A. J. Gillissen, P. J. M. Stals, A. R. A. Palmans, E. W. Meijer, *Chem. Eur. J.* **2012**, 18, 11761-11770.

[13] a) J. Matern, Y. Dorca, L. Sánchez, G. Fernández, *Angew. Chem. Int. Ed.* **2019**, *58*, 16730-16740 and references therein; b) S. Ogi, V. Stepanenko, K. Sugiyasu, M. Takeuchi, F. Würthner, *J. Am. Chem. Soc.* **2015**, 137, 3300-3307; c) S. Ogi, V. Stepanenko, J. Thein, F. Würthner, *J. Am. Chem. Soc.* **2016**, 138, 670-678; c) O. Shyshov, S. V. Haridas, L. Pesce, H. Qi, A. Gardin, D. Bochicchio, U. Kaiser, G. M. Pavan, M. Von Delius, *Nat. Commun.* ***2021***, *12*, 3134; d) J. S. Valera, R. Gómez, L. Sánchez, *Small* ***2018***, *14*, 1702437; e) J. Matern, Z. Fernández, N. Bäumer, G. Fernández, *Angew. Chem. Int. Ed.* **2022**, *61*, e202203783; f) S. Ogi, K. Matsumoto, S. Yamaguchi, *Angew. Chem. Int. Ed.* **2018**, *57*, 2339-2343; g) Q. Huang, N. Cissé, M. C. A. Stuart, Y. Lopatina, T. Kudernac, *J. Am. Chem. Soc.* **2023**, *145*, 5053-5060.

[14] C. B. Whitehead, M. A. Watzky, R. G. Finke, *J. Phys. Chem.C* **2020**, *124*, 24543-24554.

[15] G. Meisl, J. B. Kirkegaard, P. Arosio, T. C. Michaels, M. Vendruscolo, C. M. Dobson, S. Linse, T. P. Knowles, *Nat. Protoc.* **2016**, *11*, 252-272.

[16] C. Poidevin, G. Duplaix-Rata, K. Costuas, A. Fihey, *J. Chem. Phys.* **2023**, *158*, 074303.

Entry for the Table of Contents

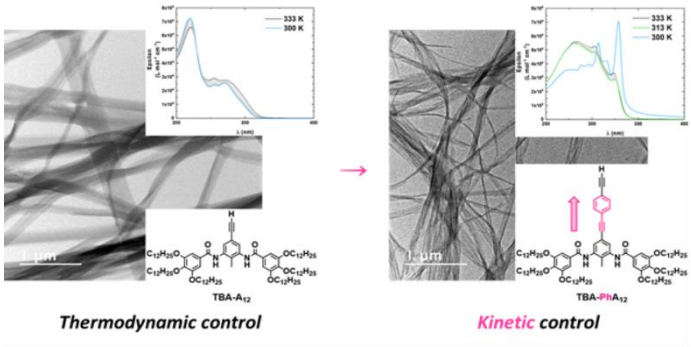

We demonstrate how proper molecular engineering can open new opportunities to create kinetically metastable states in monomers undergoing cooperative supramolecular polymerizations, by favoring dispersive interactions over H-bonds and thereby rebalancing the interplay between π- π stacking, Van der Waals and hydrogen bonding interactions.

Institute and/or researcher Twitter usernames: @chimie_ISCR / @GalangauO